Review of Support Interference in Dynamic Tests

L. E. Ericsson and J. P. Reding
Lockheed Missiles and Space Company, Inc., Sunnyvale, California

Introduction

THE problem of support interference has, of course, existed as long as the wind tunnel. Although numerous investigations of support interference have been performed since the one reported by Perkins,[1] very few review reports have been published. The well-known one by Whitfield[2] only considered the effects of the support in static wind tunnel tests. In this paper, the early work on static support interference will be reviewed very briefly before going into the more complex present-day problems, i.e., dynamic support interference and the special problems associated with static and dynamic tests at very high angles of attack.

Model Support

In most wind tunnel tests* the model has to be held in place by a support. Figure 1 shows examples of the different types used. The wire-suspension method (Fig. 1a) is, for all practical purposes, restricted to low-speed testing, whereas the strut and sting supports alone (Figs. 1b and 1c) or in combination (Fig. 1d), are used at all speeds. Although all of the support methods will be discussed, the main emphasis will be placed on the sting support system, as it is by far the most common.

The discussion will first focus on testing at moderate angles of attack, starting with static support interference before going into the more difficult problem of dynamic support interference. The special difficulties encountered in static and dynamic tests at very high angles of attack will be dealt with last.

Static Support Interference

According to Whitfield,[2] the supersonic sting support problem was first pointed out by Perkins[1] for continuum flow, and by Kavanau[3] for rarefied flow conditions. Whitfield's review will be used as the starting point before discussing more recent results.

Sting Support

The sting interference problem for static tests at supersonic speeds was envisioned by Whitfield, as shown in Fig. 2. For a small-diameter cylindrical support, the interference comes from the downstream conic fairing (the sting flare). As shown in Fig. 2, the interference starts to occur when the sting flare has been moved forward to the body wake "throat." Thus, the critical sting length is determined by the extent of the base recirculation region. As this separated flow extent is strongly dependent upon where boundary-layer transition occurs,[4] the critical sting length is very sensitive to the transition location (Fig. 3).

When the flow is completely laminar, with transition well downstream of the wake throat, the critical sting length increases with increasing Reynolds number[3] (Fig. 4), in complete agreement with the *Re* trends for the extent of laminar flow separation.[4,5] When transition occurs in the near wake, the trends with Reynolds number are reversed[1,3] (Fig. 5), exactly as for transitional boundary-layer separation.[4,5] When transition occurs well up on the body, the critical sting length is very small, but does increase with increasing Reynolds number (Fig. 5), in agreement with the *Re* trends for turbulent flow separation.[4,5]

In addition to Reynolds number, Mach number also has a strong effect on the critical sting length. The M trends for the separated flow extent for backward-facing steps[6] and near wakes[7] make one expect the critical sting length minimum at $M \approx 4$. This Mach number trend is displayed by Kavanau's results (Fig. 4). The apparent reversal of this M effect at transitional wake conditions (Fig. 5) simply reflects the fact that the transition Reynolds number increases with increasing Mach number. One can visualize how the true Mach number trend will be recovered for turbulent flow (see results for $M = 3.00$ and 3.98 in Fig. 5). When increasing the Mach number above $M = 4$, one expects the critical sting length to increase and finally to level out at some hypersonic Mach number. When the Mach number is decreased from $M = 4$,

---

Lars E. Ericsson is a Senior Consulting Engineer in the Engineering Technology organization, where he acts as a consultant to Satellite and Missile Systems Divisions on problems associated with aeroelasticity and vehicle dynamics. Before joining Lockheed Aircraft Corporation in 1956, and Lockheed Missiles and Space Company in 1959, he was with the Aeronautical Research Institute of Sweden and the Swedish Aircraft Company. He received his M.S. degree from the Royal Institute of Technology, Stockholm, in 1949, and his Ph.D. in 1972. He is an Associate Fellow of the American Institute of Aeronautics and Astronautics and has published more than 100 papers in his related fields.

Pete Reding, an Associate Fellow of AIAA, has had roughly 24 years experience in the aerospace industry, working generally in the field of unsteady aerodynamics. Immediately after graduation from the University of Michigan in 1958, he worked at Douglas Aircraft Co. for 2½ years before moving to Lockheed Missiles and Space Co. in 1961, where he has wrestled with separated flows, booster aeroelastic stability, airfoil stall, the dynamics of bulbous-based bodies, ablating bodies, Shuttle vehicles, decelerators, aeroacoustics, and dynamic support interference. He has made practical contributions to the design and development of such vehicles as the Trident I missile, the Space Shuttle, the Seasat A booster, and the Saturn-Apollo boosters.

Presented as Paper 82-0594 at the AIAA 12th Aerodynamic Testing Conference, Williamsburg, Va., March 22-24, 1982; submitted March 31, 1982; revision received Feb. 21, 1983.

*The exceptions are tests in the free-flight tunnels and in facilities that use a magnetic support system.

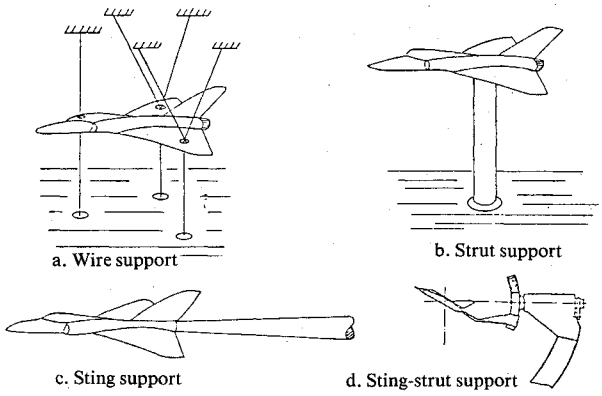

Fig. 1 Support systems.

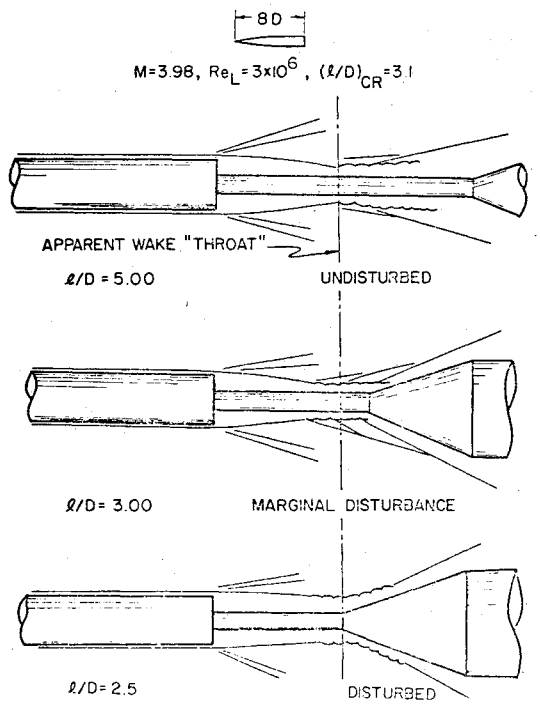

Fig. 2 Schematic of schlieren photographs of sting support flow patterns (Ref. 2).

one finds, as expected, that the critical sting length peaks out at sonic speed.[8] Later investigations[9-12] have, in general, confirmed these effects of Mach number on the critical sting length.

The concern so far has been with the large effect of the sting flare. What is the effect of the slender cylindrical sting? Stivers and Levy[13] used a thin, wide plate to split the sting in two halves, one of which they varied in size down to zero. They found their results to indicate that there is no sting diameter, no matter how small, for which the sting support interference on the base pressure disappears, at least not for the transonic Mach number range, $0.60 \leq M \leq 1.40$, that they investigated. Sieling[14] obtained similar results at $M=3.88$ in the Rutgers Axisymmetric Near-Wake Tunnel (RANT), which has a test section with a central circular cylinder, thus allowing him to investigate the effect on the base of a dummy sting with an arbitrarily small diameter. The results in Ref. 15 show that even when the effects of a cylindrical sting on the base pressure are not measurable, the base flow inside 80% of the base radius could still be appreciably disturbed. This may help to explain the fact that even if the sting support effect is negligible on the measured static stability derivatives, it can still be of significant magnitude in regard to dynamic stability data, as will be shown.

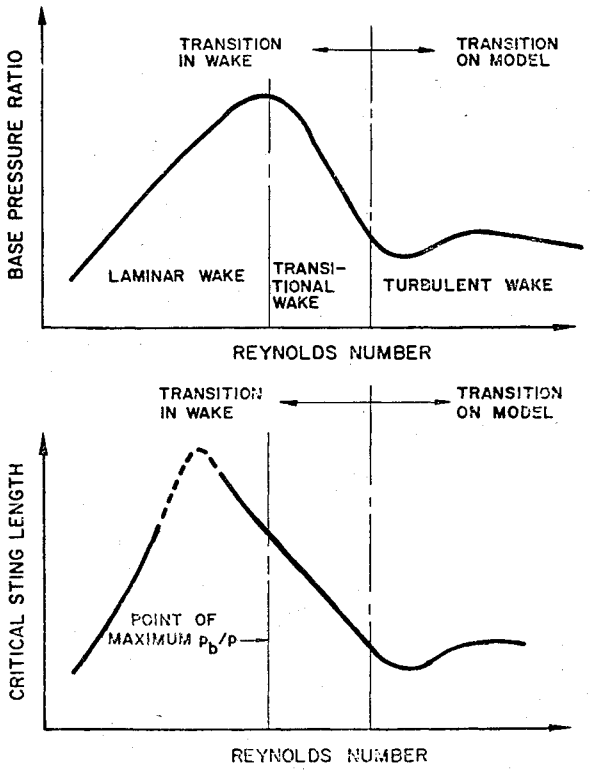

Fig. 3 Typical effect of Reynolds number on base pressure and critical sting length (Ref. 2).

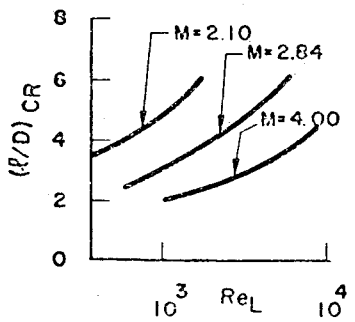

Fig. 4 Critical sting length for laminar wakes (Ref. 3).

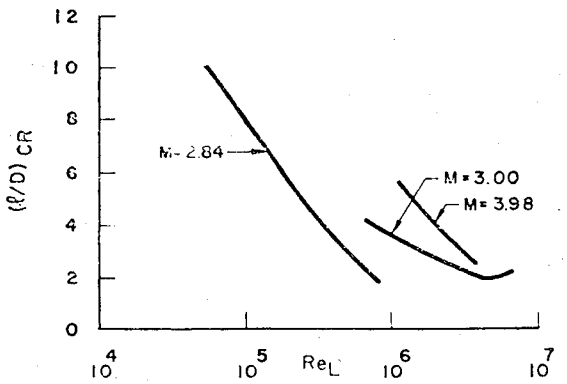

Fig. 5 Critical sting length comparison (Ref. 2).

All the results discussed so far are for a slender body with a flat base. When the body has a boat-tail or bulbous base, the support-interference problem becomes much more serious.[16] Perkins[1] found that the support interference influenced the separated flow region on the boat-tail. Thus, not only the base pressure and associated drag are affected, but also the normal force and moment characteristics[16] (Fig. 6). The difference between rod-mounted and sting-mounted models is mainly an

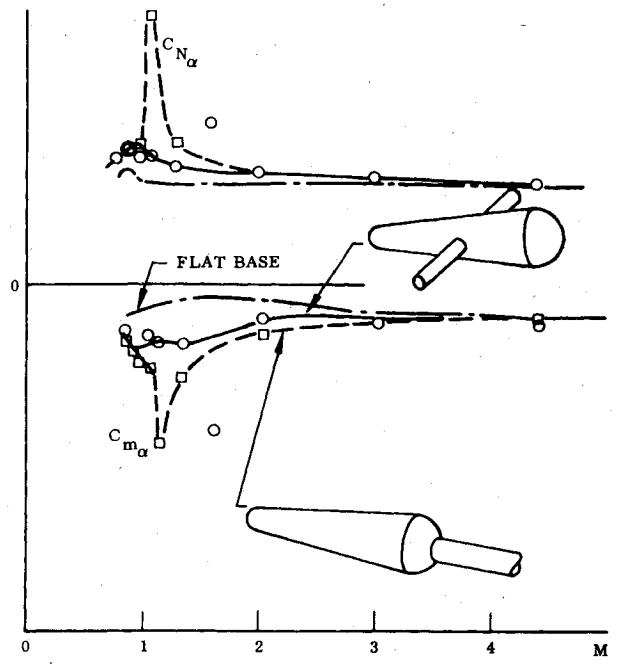

Fig. 6 Static derivatives at $\alpha = 0$ of a slender cone with hemispherical base (Ref. 16).

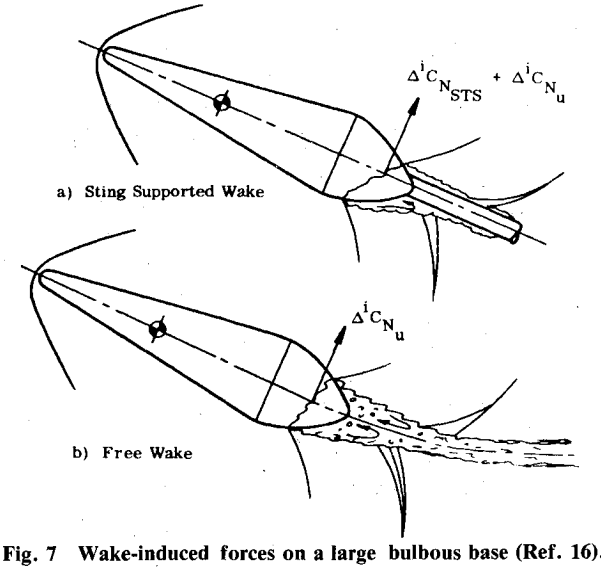

Fig. 7 Wake-induced forces on a large bulbous base (Ref. 16).

indication of the static support interference from a cylindrical sting. Thus, in the presence of a bulbous base, even a slender cylindrical sting produces significant support interference in the transonic speed region.

Comparing the results for flat and bulbous bases in Fig. 6, one finds that the base supports a positive normal force component that generates a stabilizing moment contribution. The results show further that the base force and associated stabilizing moment contribution are reinforced by the interference from the cylindrical sting. The schematic flow pictures in Fig. 7 illustrate what happens. The sting induces a positive normal force on the bulbous base by affecting the location of the flow separation. When the sting is pitched, there is an increase in the strength of the windward side recompression pressure. This increases the return mass flow rate and causes a forward movement of the windward side separation boundary on the bulbous base. Opposite effects occur on the leeward side, and a positive load is induced on the base as a result (Fig. 7a).

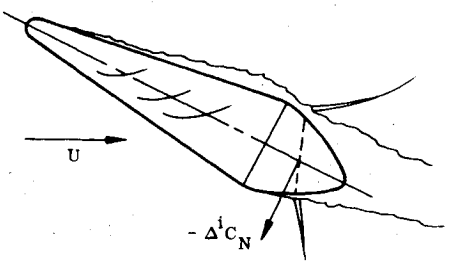

Fig. 8 Forces induced on a bulbous base by forebody cross flow (Ref. 16).

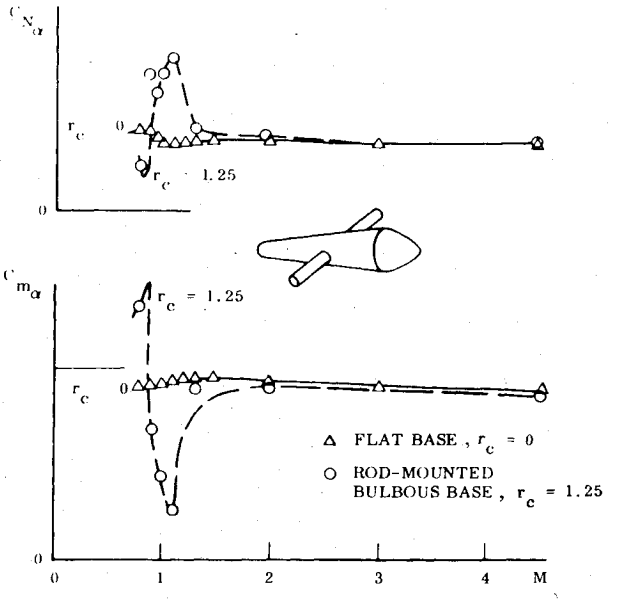

Fig. 9 Effect of large bulbous base on static derivatives of a slender cone at $\alpha = 0$ (Ref. 16).

Similar reasoning can be used to explain the positive load induced by a free wake (Fig. 7b). The flow developed on the forebody, generating a positive lift, directs the wake downward. Because the wake is gradually turned back into the freestream direction, a transverse pressure gradient exists in the wake. The higher windward side recompression pressure at the wake throat is communicated forward to the base, generating a positive normal force on the bulbous base (Fig. 7b), in the same manner as for the sting-mounted body (Fig. 7a).

The base flow and associated aerodynamic loads are also affected by viscous forebody cross flow (Fig. 8). Forebody cross flow causes the leeward side boundary layer to become thick and attain a separation-prone velocity profile. This occurs through collection of low-energy fluid, swept from the windward side. The same flow process serves to make the windward side boundary layer stronger and less separation-prone. The resulting promotion of flow separation on the leeward side and delay on the windwrd side generates a negative normal force component on the base, $\Delta^i C_N < 0$ (Fig. 8). These two opposing effects vary in relative magnitude such that the wake effects dominate in one Mach number region and forebody cross-flow effects in another (Fig. 9).

The drastic variation of the aerodynamic effects of a bulbous base between $M = 0.8$ and 1.2 in Fig. 9 can be explained as follows: Figure 10 shows how the base pressure and minimum body surface pressure vary with Mach number on slender cones and cone-cylinder bodies.[17-19] It is clear that at subsonic speeds a sizable compression is needed to get from the body shoulder pressure to the base pressure. Such an adverse pressure gradient will cause the flow to separate ahead of the base,[20-22] as is illustrated in the top left insert in Fig.

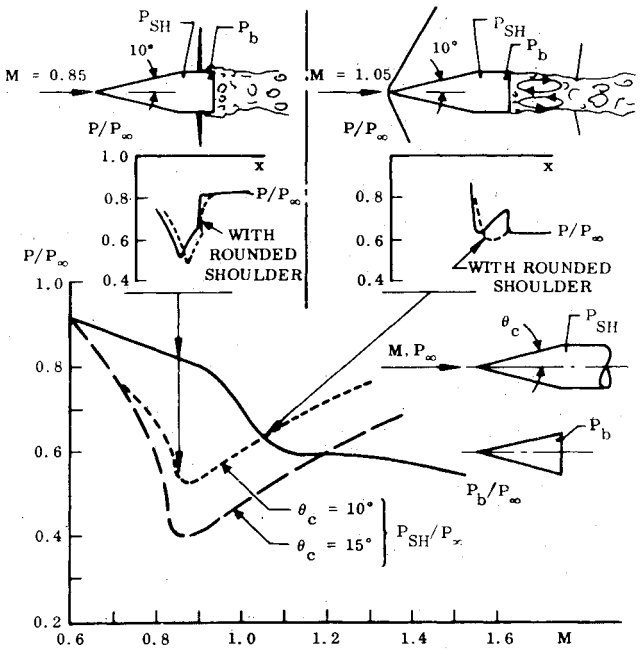

Fig. 10 Pressure distributions and flow patterns over slender cone-cylinder configurations at transonic speeds (Ref. 16).

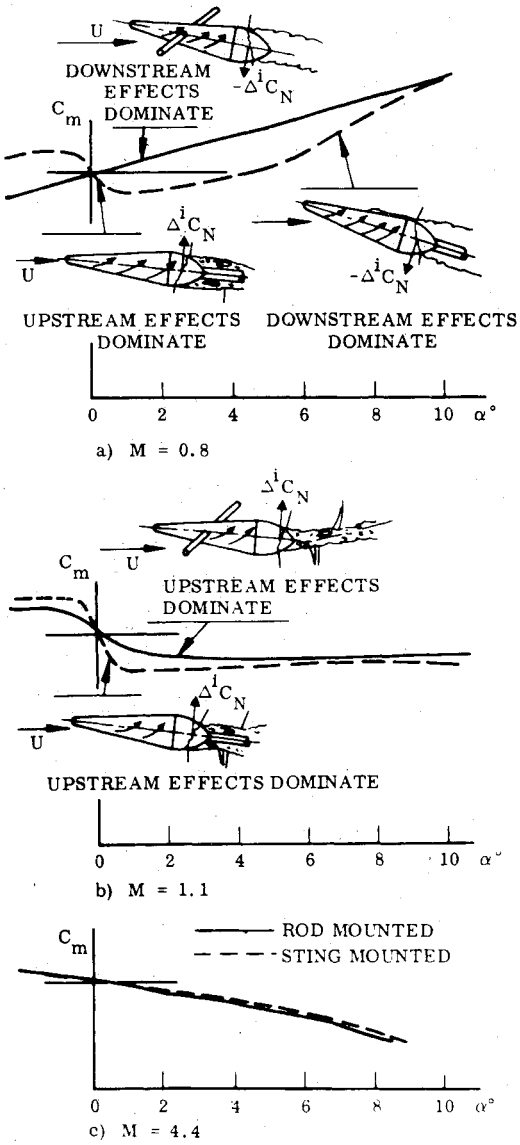

Fig. 11 Sting interference effects on static stability characteristics of a slender cone with a large bulbous base (Ref. 16).

10. The strength of the shock is affected by the wake via base pressure changes. The base pressure change due to angle of attack is small compared to the pressure rise through the shock. Thus the upstream communication effect from the wake recompression region will be small, and the main contribution to the force on the bulbous base will be generated by forebody cross-flow effects. Hence one can expect the large, rounded base shoulder to have a statically destabilizing effect, in agreement with the results in Fig. 9.

Returning to Fig. 10, it appears that minimum compression is needed between shoulder and base pressure when the Mach number is slightly supersonic ($M \approx 1.05$ for $\theta_c = 10$ deg). This situation is depicted in the top right inset of Fig. 10. In this case, with no terminal shocks on the body, a more direct communication with the wake exists. Hence the upstream wake effect will dominate, and one can expect the large bulbous base to have a statically stabilizing effect, in agreement with the supersonic data trend in Fig. 9.

How the sting can distort this balance between downstream and upstream viscous flow effects is illustrated by the experimental results[16] in Fig. 11. At $M = 0.8$, the dominance of the forebody cross-flow effects is truthfully represented by the test results for the rod-mounted model. The sting, however, reinforces the wake recompression effects so much that they dominate at low angles of attack. Also, at $M = 1.1$, where the upstream wake communication effects dominate for the free and rod-mounted body, the sting shows this strong reinforcement of the wake recompression effect. As the Mach number is incresed, the sting support interference gradually decreases and has practically disappeared at $M = 4.4$.

Other Support Systems

Another common way to support the model is by the use of a strut support. It has been used successfully, especially in regard to the testing of aircraft models. However, it can have a strong effect on the pressure distribution on an aircraft fuselage or a slender body, as is demonstrated by the results obtained by Ruben.[23] Perkins[1] showed the strut interference to be large for a boat-tailed slender body. In that case, the support interference is enhanced by the interaction between the strut wake and the separated flow over the bulbous base. This is similar to the interference from the rod wake for a rod-mounted model[16] (Fig. 12). Similar adverse effects of strut supports have also been reported for aircraft models.[24-26]

A wire support system investigated by Gray[27] and also reported by Whitfield[2] was found to have a large interference effect on the flow over a boat-tailed blunted cone.

Dynamic Support Interference

Steadily increasing performance demands expose present-day aerospace vehicles to unsteady flowfields which generate

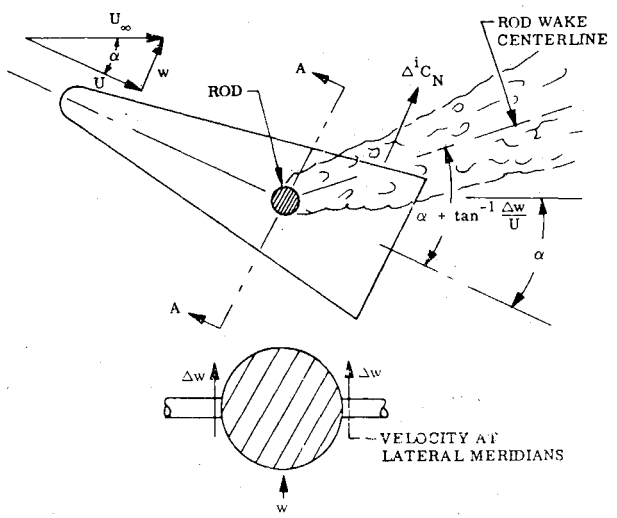

Fig. 12 Rod wake interference at large angles of attack (Ref. 16).

highly nonlinear aerodynamics that exhibit significant coupling between longitudinal and lateral degrees-of-freedom. The complex vehicle dynamics are caused by separated flow effects of various types, which have largely eluded theoretical description and, therefore, are placing great demands on dynamic testing capabilities.[28] Many flow separations occur only at high angles-of-attack. However, one type, the base flow recirculation, is present at all angles and induces strong support-interference effects for models oscillating around small angles-of-attack or yaw.

The support interference is more of a problem in dynamic than in static tests. To begin with, the support system is often much bulkier than in static tests. This is because of the increased demands on rigidity. In the static test, the effects of sting vibrations are usually time-averaged out to have a negligible effect on the experimental results. In dynamic tests, however, the sting oscillation presents an additional, unwanted degree-of-freedom of the model motion. In the case of forced oscillations, the support system must house the driving mechanism, further increasing the size requirements.

Even if the support dimensions were the same in static and dynamic tests, the support interference would affect the data accuracy much more in the dynamic than in the static case. The reason for this is twofold. The relative motion between model and support increases the effect of the support interference on the moment derivative $C_{m\alpha}$. In addition the measured phase relationship, which relates the static derivative $C_{m\alpha}$ to the dynamic derivative $C_{mq}+C_{m\dot{\alpha}}$, is severely distorted by the support interference. As a result, it is not unusual to find the support-interference effect to be one order of magnitude larger for $C_{mq}+C_{m\dot{\alpha}}$ than for $C_{m\alpha}$.[29]

Symmetric Slender Sting

The cylindrical sting presents the simplest example of this support category. As was discussed earlier, the cylindrical

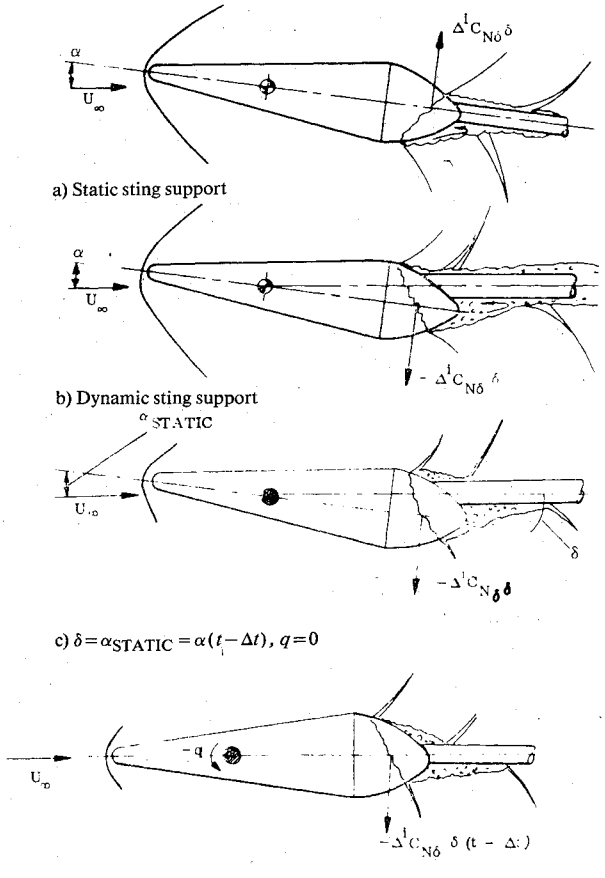

Fig. 13 Sting-induced forces on a bulbous base (Ref. 29).

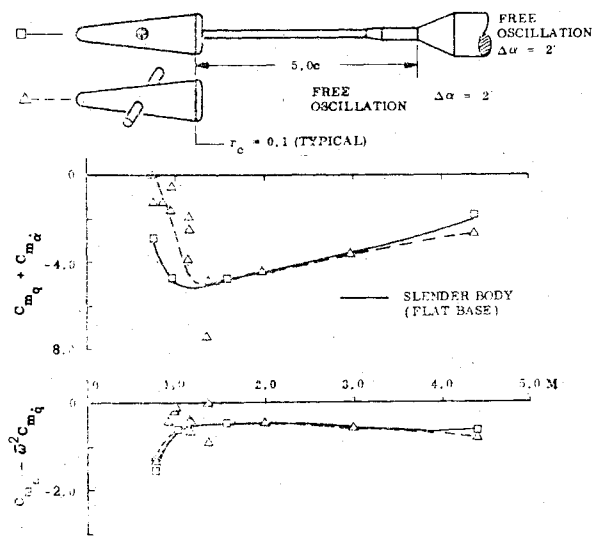

Fig. 14 Effect on mounting method on dynamic stability of a bulbous-based slender cone (Ref. 16).

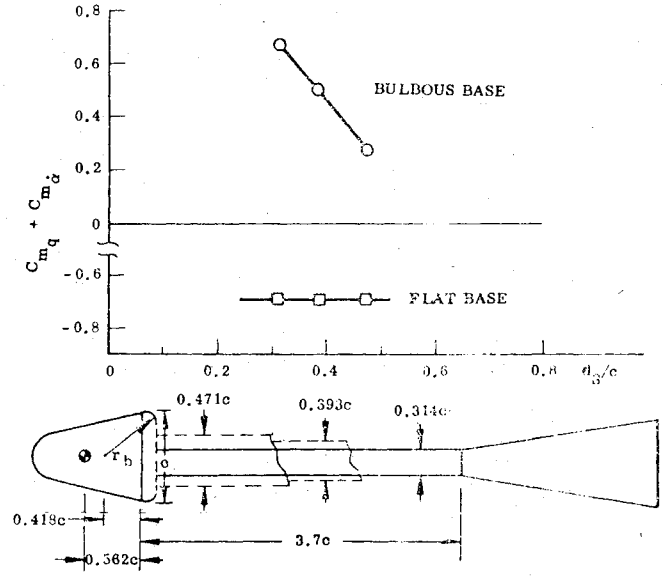

Fig. 15 Effect of sting diameter on the damping of a bulbous-based cone at $M=0.65$ (Ref. 30).

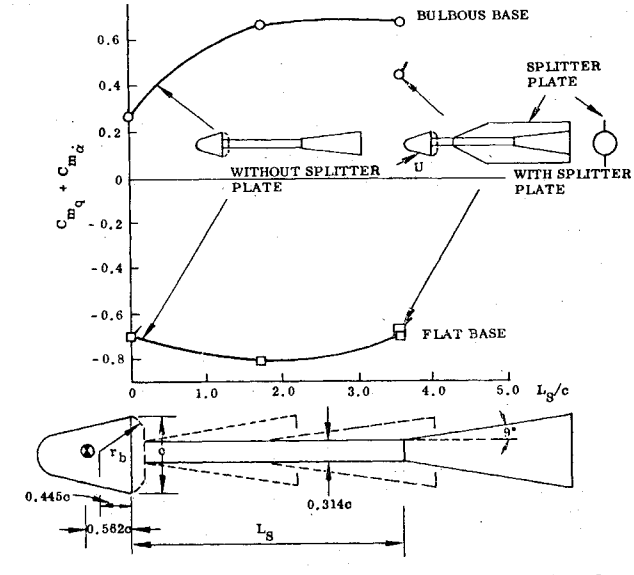

Fig. 16 Effect of sting flare on the damping of a bulbous-based cone at $M=0.65$ (Ref. 30).

sting reinforced the upstream wake recompression effect in static tests. In the dynamic case, the support interference is quite different,[29] as is illustrated in Fig. 13. As the model pitches relatively to the sting, the interference from the dynamic support will be negative, statically destabilizing, i.e., the opposite of what it is in a static test (compare Figs. 13a and 13b). When the rotation center is well forward of the base, which usually is the case, base plunging relative to the sting amplifies the dynamic support-interference effect.

For the oscillating model, the interference load lags the vehicle motion due to the time Δt required for convection downstream to the wake neck and back to the base through the recirculation region. Thus a residual interference load occurs, as the body pitches downward through $\alpha = 0$, which opposes the motion (compare Figs. 13c and 13d). Consequently, the dynamic sting interference produces an erroneous, often very unconservative measure of the damping of bulbous-based bodies, as is demonstrated by the results in Fig. 14. They also illustrate the fact alluded to earlier, i.e., the sting-induced effects on $C_{mq} + C_{m\dot{\alpha}}$ are very much larger than those on $C_{m\dot{\alpha}}$.

The data in Fig. 14 illustrate further that at high subsonic speeds even a modest amount of shoulder roundness is enough to allow the wake recompression effects to propagate forward of the base. At supersonic speeds, the very slender sting causes no interference; and for a flat-based model, it causes none at any speed. Thus the figure illustrates amply how base roundness aggravates the problem of support interference. One is tempted to conclude that, as in the case of the interference effect on base pressure[13,14] discussed earlier, there is probably no sting diameter small enough to eliminate completely the subsonic dynamic support interference for a model with a rounded base shoulder. Wehrend's results[30] seem to support this, as there is no "plateauing" tendency with decreasing sting diameter (Fig. 15).

Wehrend[30] showed that a symmetric, slender flare could reinforce the damping interference effect of a cylindrical sting (Fig. 16). Similar results have been obtained for a flat-based cone at supersonic speeds (Fig. 17). Adding a splitter plate to the sting support also has a damping interference effect for the bulbous base, but has no effect in the case of a flat-based model.[9-12,30] Apparently, the splitter plate deforms the wake and cannot be used when testing bulbous-based bodies.

When the model consists mainly of the bulbous base itself, as in the case of the Viking re-entry configuration, one can, of course, expect the support interference to become especially large. The problem is well illustrated by experimental results,[31,32] both in regard to the effect of sting diameter (Fig. 18a) and the effect of the distance to a 20-deg sting flare (Fig. 18b). Use of a sting support can completely mask the wake-induced negative aerodynamic damping if great care is not exercised. It is obvious that the true level of negative damping for the Viking configuration cannot be ascertained from the dynamic tests performed.[31,32] It should be emphasized that even when the dynamic sting support effects are as large as is shown in Fig. 18, the effects on static results can still be negligibly small.[33,34]

It is clear from the discussion so far that it is practically impossible to avoid dynamic sting interference when the model has a boat-tail or rounded base shoulder. For a model with a flat base, sting support interference is usually not a problem. There are, however, two exceptions: 1) tests conducted at hypersonic, low-density flow conditions, which will be discussed more in the following section; and 2) tests conducted at a Reynolds number such that boundary-layer transition occurs on the aft body near the base.[35]

It is shown in Ref. 35 that transition does occur on the body near the base, and that the transition-augmented support-

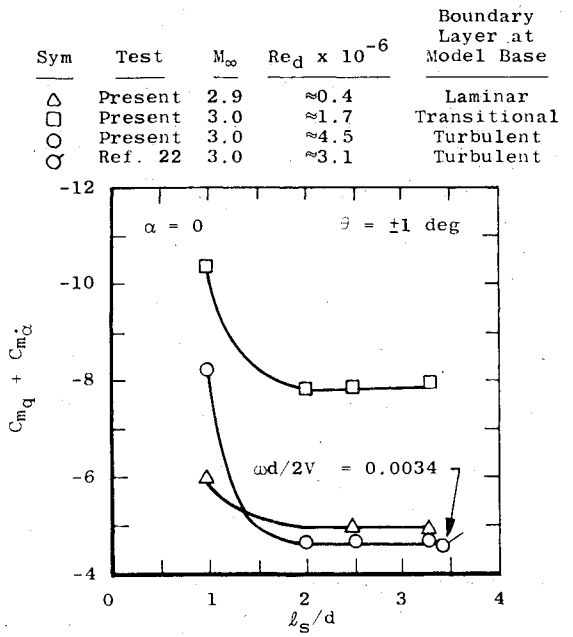

Fig. 17 Effect of sting length on the damping of a flat-based 7-deg cone (Ref. 9).

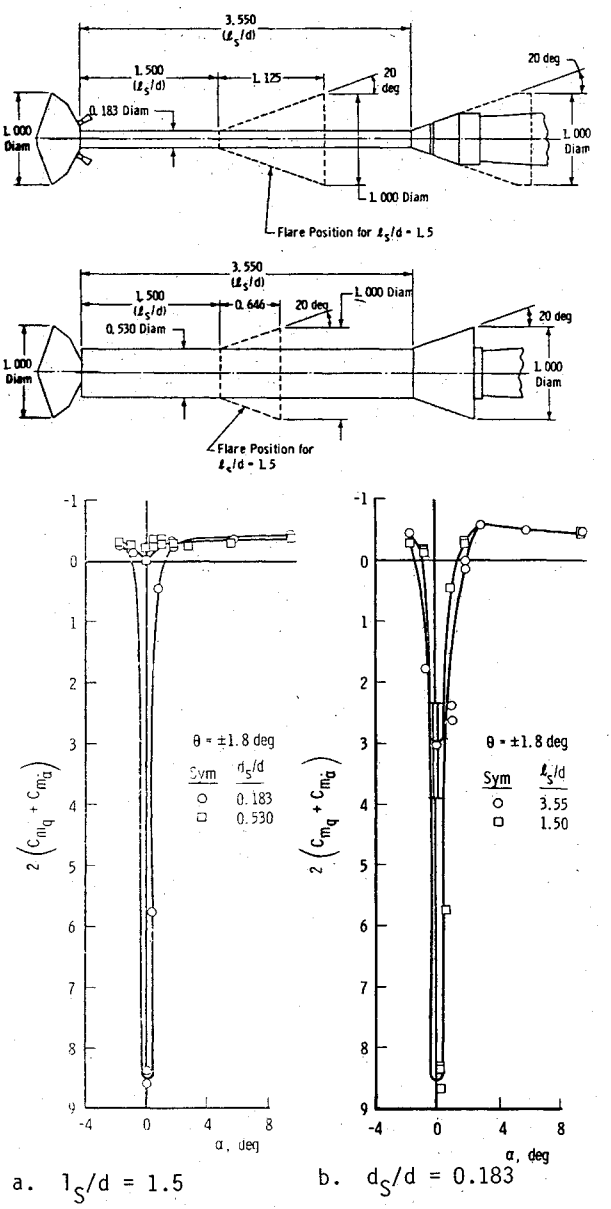

Fig. 18 Effect of sting diameter and sting length on the damping of the Viking configuration (Ref. 31).

interference effect measured by Wehrend[30] can be computed from static data. Figure 19 shows that when the damping data are corrected for the sting interference they agree well with other experimental results[36] and with theory.[37] Similar transition-augmented sting interference has been documented by Orlik-Rückemann et al.[38] at $M=2$ for a 7.5-deg cone (Fig. 20).

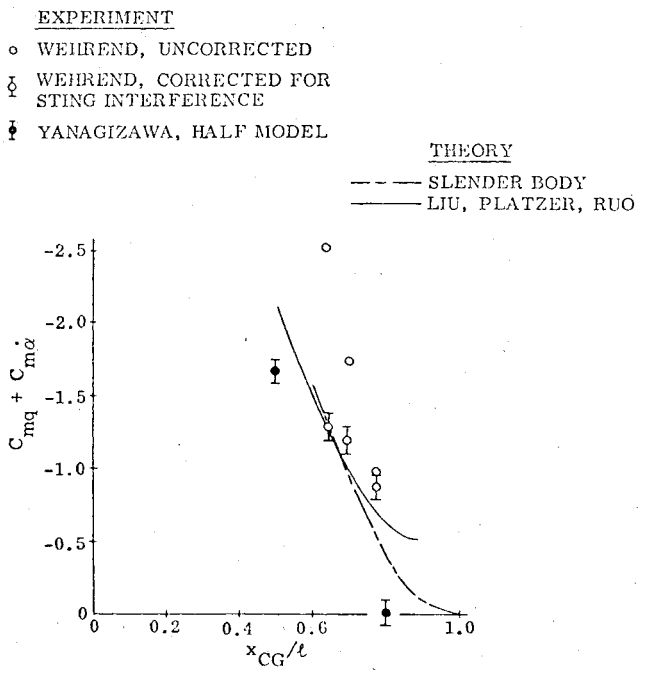

Fig. 19 Damping of a 12.5-deg sharp cone at $M=1$ for various rotation centers (Ref. 38).

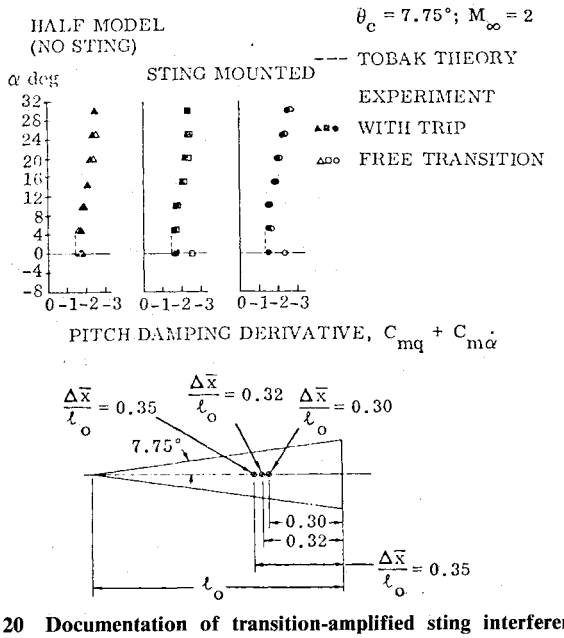

Fig. 20 Documentation of transition-amplified sting interference (Ref. 38).

Asymmetric Support

Figure 21 shows the asymmetric slender sting used by Adcock[39] to obtain the results in Fig. 22. The opposite data trends for $C_{mq}+C_{m\dot{\alpha}}$ and $C_{m\alpha}$ are apparent, indicating the dominating base recirculating effects on the bulbous-based models. The strong correlation between $C_{m\alpha}$ and $C_{m\delta}$ indicates that much of the wake-induced load on the bulbous base is generated by support interference. The interference derivative $C_{m\delta}$ was obtained in static tests by deflecting the sting the angle δ_S relative to the model (Fig. 21) and pitching the model-sting combination. The results were then carpet-plotted[40] (Fig. 23) to yield the interference derivative $C_{m\delta}$. The sign of the interference derivative, $C_{m\delta}<0$, indicates that the dynamic interference effect of the slender asymmetric sting (Fig. 23) is the opposite of that of a slender symmetric sting, i.e., it is undamping.

Figure 23 shows that the effect of sting deflection δ_S is highly nonlinear, with a more or less discontinuous C_m change between $\delta_S=0$ and -1 deg. As the sting is pitched to the windward side, $\delta_S<0$, its leeward side becomes more deeply submerged in low-energy wake flow. The windward side reattachment pressure increases relative to the leeward side until it, through the upstream communication, flips the wake to the leeward side (as described in Refs. 28 and 29). Therefore a negative base load and a discontinuous, statically destabilizing increase in the pitching moment result (Fig. 23).

At low subsonic Mach numbers, the negative force results not only from the differential separation and associated pressure differential over the base, which is the mechanism at transonic speeds, but from differential pressures propagated forward of the base as well. The asymmetric sting flare directs the wake downward at $\alpha=\delta_S=0$, causing a positive base load and an associated strongly stabilizing pitching moment (Fig. 23). It is obvious from the earlier discussion of Fig. 13 that the statically stabilizing support-interference effect in Fig. 23 will be undamping, accounting for much of the measured large undamping in Fig. 22. References 16 and 29 describe how experimental results, such as those in Fig. 23, can be used to correct the experimental data for the asymetric sting interference, giving the corrected data shown in Fig. 24.

In hypersonic low-density flow, even a flat-based model experiences sting support interference, as a thick boundary layer opens up the communication between aft body and wake. The presence of the support affects the lip shock via the wake recompression pressure, propagated upstream through the near-wake recompression region. The resulting change of shoulder pressure is felt upstream of the base to an extent roughly proportional to the boundary-layer thickness.[41] At high Mach numbers and very low Reynolds numbers, the lip and wake recompression shocks appear to merge,[41] allowing the sting to affect the lip shock almost directly. This explains why the nonlinear damping results of Hobbs for a flat-based cone[42,43] bear such similarity to the subsonic results for the bulbous-based cone[39] (Fig. 25). The asymmetric flared sting has very similar effects in the two cases, causing a large decrease of the damping at $\alpha=0$, where the wake flipping has its largest effect (Fig. 23).

Another rather common, asymmetric sting-strut arrangement, used in hypersonic dynamic tests, is the one investigated by Walchner et al.[44,45] (Fig. 26). The asymmetric sting-strut juncture causes divergent oscillations when it is too close to the model base. The base pressure variation for the short sting (Fig. 27) shows that at $\alpha=6.2$ deg, where the

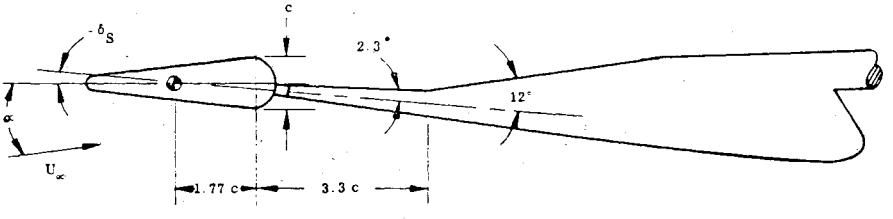

Fig. 21 Asymmetric sting and bulbous-based model (Ref. 39).

oscillations started (Fig. 26), the measurements gave $p_B > p_\infty$ rather than the expected $p_B < p_\infty$. The sting-strut juncture acts as the sabot in Ref. 46, opening the wake (see flow sketch in Fig. 27) to produce a base pressure reading of $p_B/p_\infty > 4$. The flow sketch illustrates how this pressure rise will be propagated over the windward side base shoulder to produce a positive, statically stabilizing aft body load. Due to the time lag effect it will be dynamically destabilizing, thus accounting for the initial divergence of the oscillations in Fig. 26. When the amplitude has increased to produce $\alpha_0 + \Delta\theta > 6.25$ deg, the wake is "flipped," as illustrated in the flow sketch (Fig. 27), producing a loss of shoulder pressure on the top side and resulting in a discontinous increase of the aft body load. The discontinous increase of static stability corresponds to a discontinuous decrease of damping, explaining the sudden amplitude increase in Fig. 26.

The pressure data for the long sting, $l_S/d = 4.2$, also show large discontinuous changes of base pressure (Fig. 28), rather similar to those for the short sting. Why, then, are not the oscillation traces also similar (Fig. 26)? The answer lies in the fact that the initial release angle, $\alpha_0 + \Delta\theta = 6.1$ deg, was, in the case of the long sting, enough to flip the wake, and a close to normal (support-free) near wake was established (see sketch in Fig. 28). The oscillations never dipped below $\alpha_0 - \Delta\theta = 1.9$ deg and could not, therefore, catch the base pressure discontinuity in the return loop at $\alpha = 1.5$ deg (Fig. 28).

When the sting-strut juncture was faired over with a splitter plate, the base pressure variation for the long sting was close to the one expected for a free wake[45] (Fig. 29). Thus one would expect essentially interference-free dynamic data for this sting arrangement. Test data with a faired, shorter sting-strut arrangement confirms this.[47]

A compilation of experimental results for 10-deg sharp cones[48] contains several examples of dynamic support interference at hypersonic speeds. It could be shown[49] that the

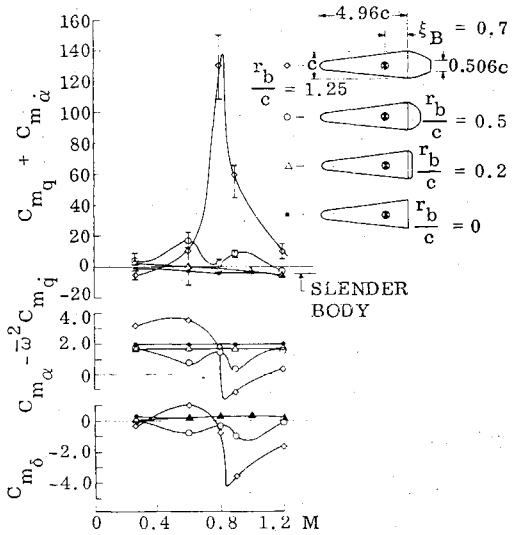

Fig. 22 Correlation of sting-support-induced moment derivative with static and dynamic stability derivatives (Ref. 16).

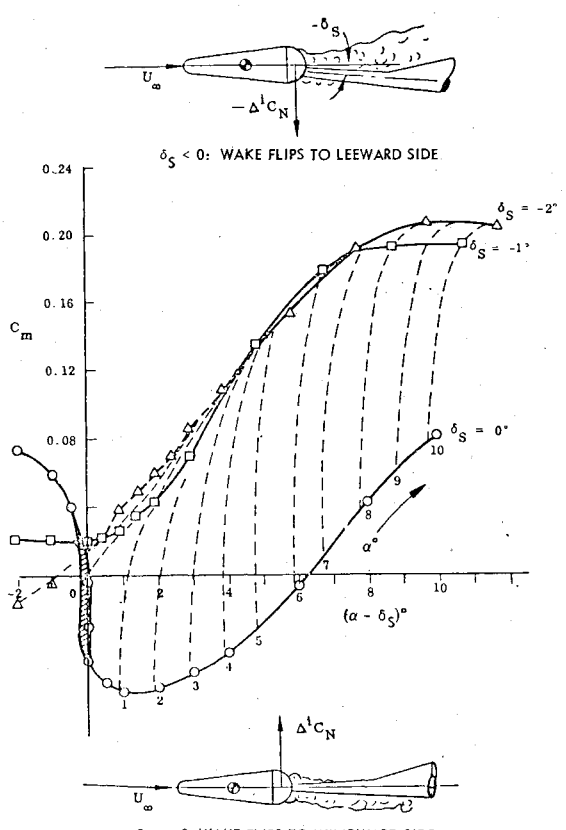

Fig. 23 Pitching moment carpet plot for $M = 0.26$ (Ref. 16).

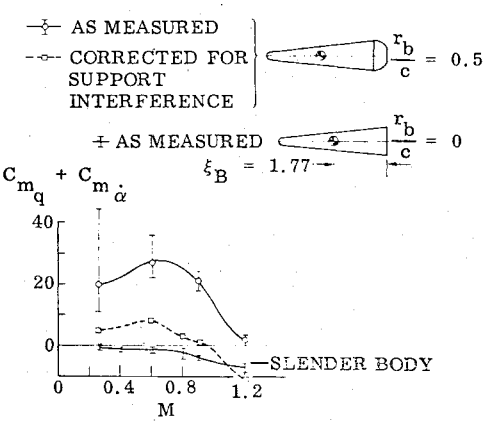

Fig. 24 Damping of hemispherical-based cone corrected for support interference (Ref. 29).

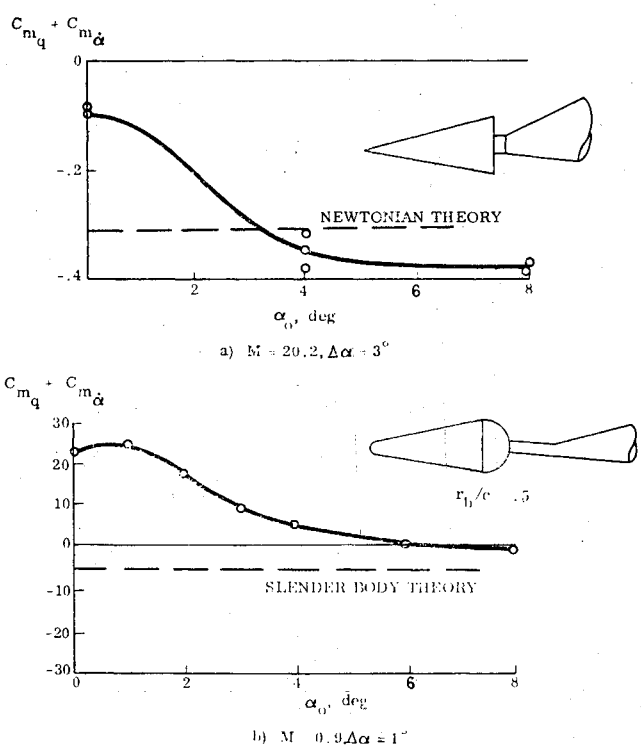

Fig. 25 Comparison of hypersonic and transonic asymmetric sting interference (Ref. 29).

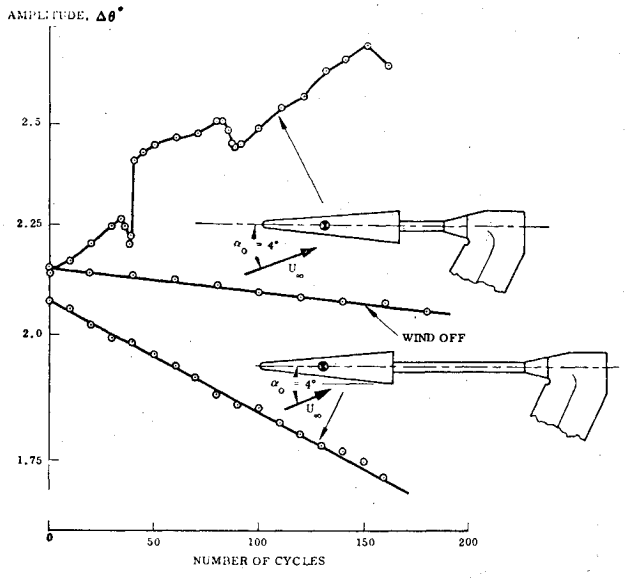

Fig. 26 Hypersonic dynamic support interference at $M=14$ (Ref. 44).

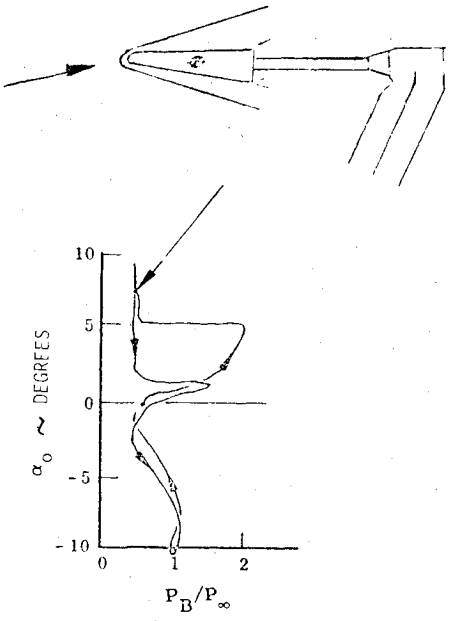

Fig. 28 Asymmetric support interference on slender cone base pressure at $M=14$, long sting.

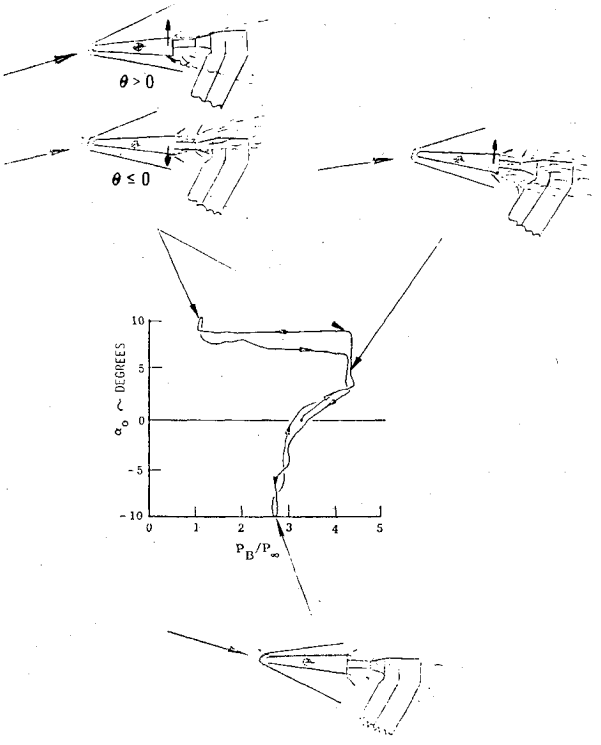

Fig. 27 Asymmetric support interference on slender cone base pressure at $M=14$, short sting.

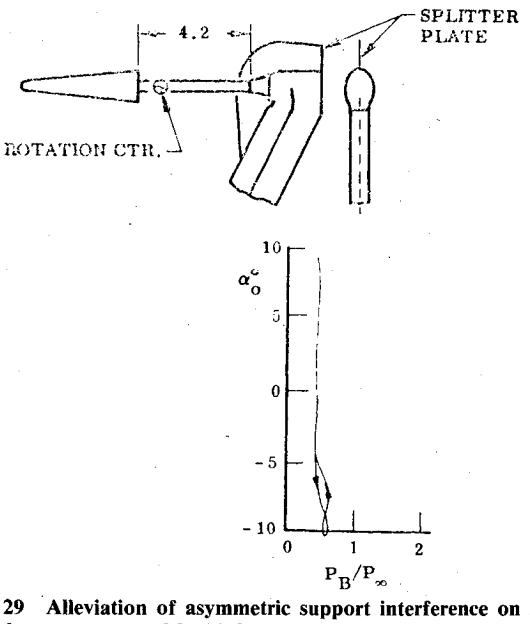

Fig. 29 Alleviation of asymmetric support interference on slender cone base pressure at $M=14$ through the use of a splitter plate (Ref. 45).

loss of damping at very high Mach numbers obtained in various wind tunnel tests[50-52] was a result of the undamping effect of the asymmetric sting-strut support systems used and could not be caused by mechanical support damping[53] that was not accounted for.

From the evidence examined, it is clear that all asymmetric sting-strut arrangements produce a strong source of support interference. The asymmetry forces a large nonlinear, often discontinuous, flow change to take place near $\alpha=0$, where most tests are performed. Judging by the results obtained by Walchner et al.[44,45,47] (Figs. 28 and 29), extending the strut all the way, to obtain a symmetric sting-strut arrangement, should alleviate and possibly eliminate the support interference from the sting-strut juncture. It should be possible to avoid dynamic support interference for flat-based models in this manner. However, based upon the experience with slender sting supports, discussed earlier, one doubts that this will eliminate support interference for a bulbous-based model. The use of splitter plates or symmetric strut arrangements will change the wake, preventing measurement of the free-wake effects on a bulbous-based model.

The openings in the base, needed to permit the relative sting movement, will also hinder the measurement of true bulbous-base effects.[54] It has been shown by Wehrend[55] that the undamping effect of a bulbous base can be all but eliminated by providing the base contour with flow fences that cut off the communication between aft body and near wake. A concave base or a base lip could perform the same task. The concave base increases the base pressure, decreasing the drag.[56] One has reason to believe that the base pressure level on the inside of the lip is rather insensitive to angle of attack. The exception appears to be when boundary-layer transition occurs in the

near wake. As the transition is sensitive the forebody cross-flow effects,[57] the transition location in the near base flow region is sensitive to α. Thus, through the strong effect of transition location on base pressure,[4] differential lip pressures are established. The resulting force is statically destabilizing and damping according to the scant experimental evidence available.

Other Dynamic Support Systems

One obvious solution to the problem of sting support interference is to use a transverse rod support. However, Dayman[49] has shown that at $M=4.64$ a wire support, located at the midpoint of a 30-deg cone, shortens the near-wake recirculation region. Since this effect disappeared when the Mach number was decreased to $M=2.02$, one is led to speculate that the interaction from the wire or rod shock with the base flow may affect the wake geometry. This would explain the Mach number sensitivity found by Dayman.[58] The rod interference would be similar to the rod wake/base wake interaction (Fig. 12), causing a local dynamic pressure reduction over the leeside base-shoulder region, thereby generating a positive, statically stabilizing normal force. Because of time lag effects, the interference effect would be dynamically destabilizing.

A direct measurement of the transverse rod interference is hard to find. Usually one can only compare rod data with sting data. This, however, may not be as futile as it appears. For example, transonic and supersonic data in Fig. 30 reveal that the measured dynamic stability differs little for a flat-based model whether or not a rod or a sting support is being used, whereas the support system did make a difference when the model had a rounded base shoulder (Fig. 14). Experimental evidence indicates that the very slender sting support used should not have any interference effect on the flat-based model. And if there were any, it should be dynamically stabilizing, as has been illustrated earlier. At transonic speeds, only the rod wake effect is present, which for small amplitude oscillations at $\alpha=0$ has little chance to spread from the lateral meridian to influence the normal force and pitching moment.

As the difference between rod- and sting-mounted data in Fig. 30 goes the wrong way, statically destabilizing and damping rather than the expected opposite rod interference trend, one can conclude that there is no rod interference for the flat-based model at $M\leq 2$. Adding base-shoulder roundness should not affect the rod interference appreciably, whereas it is known to have a very large effect on the slender sting interference. Thus the results in Fig. 14 indicate that the true undamping wake recirculation effect was measured with the rod-mounted model. Because of the large time lag for the base recirculation effect itself and its sting-induced perturbation, the dynamic data show clearly the sting-induced damping, whereas no distinct data trend can be resolved from the static data.

At hypersonic speeds, the rod interference becomes significant, as has been shown by Hobbs[32,33] (Fig. 31). A significant, dynamically destabilizing effect of the rod support[42,43] is observed until turbulent base flow conditions are reached, when all support-interference effects become small, as has been illustrated (Fig. 3). There are several reasons for the increasing rod interference at hypersonic speeds. In addition to the emergence of rod shock effects, the rod wake interference is enhanced by large boundary-layer effects on the aft body. Whereas the inviscid stream lines may obtain twice the freestream flow inclination on the body, the viscous flow can produce four times the freestream angle of attack at hypersonic speeds.[59]

At higher angles of attack and/or amplitudes, the rod interference will, of course, become important at all speeds, as the effects of the rod wake are no longer restricted to the lateral meridian. A flat-based sting-mounted model shows no effect from varying the oscillation amplitude from 2 to 10

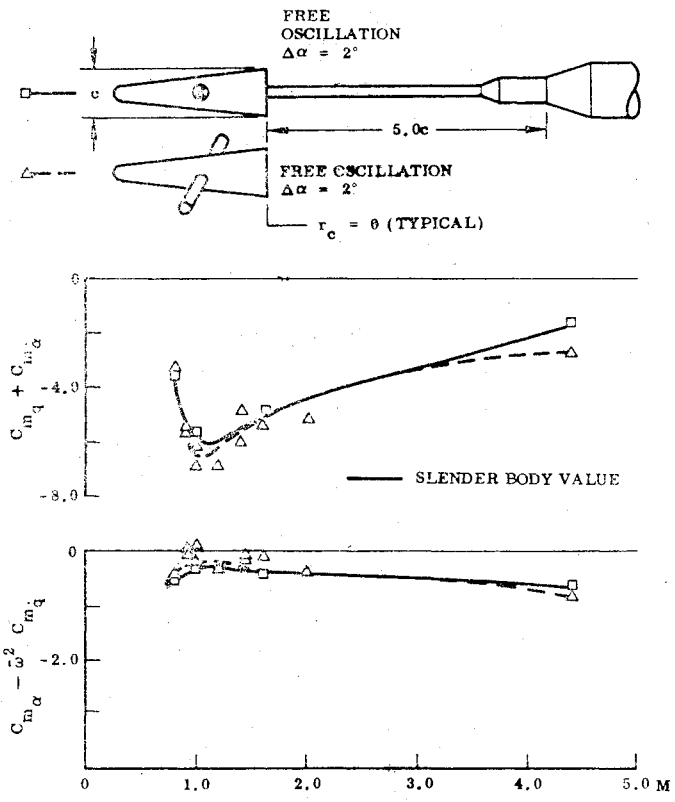

Fig. 30 Effect of model mounting on dynamic stability of a flat-based cone.

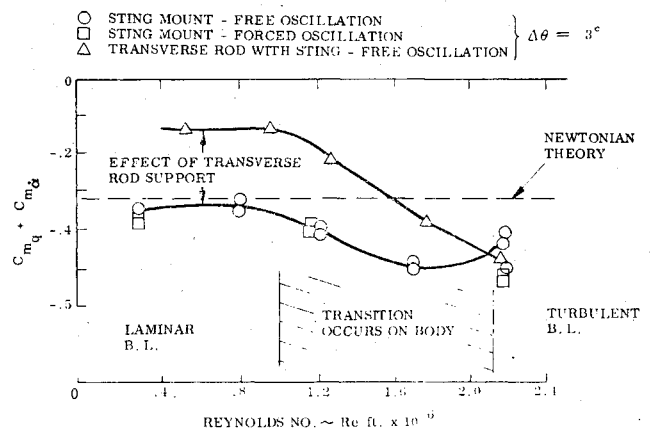

Fig. 31 Transverse rod interference at $M=10$ (Ref. 42).

deg, whereas the rod-mounted model shows a very large effect (Fig. 32). This is a clear indication of rod interference. At transonic speeds, one does not expect any nonlinear amplitude effects for a flat-based model. The measured rod effect is to increase static stability and decrease damping, all in agreement with the expected rod support-interference effect.

In addition to this $\alpha=0$ case, the rod support is also a poor choice for a short, blunt body, such as the Viking configuration discussed earlier (Fig. 18). The wire support interference for a boat-tailed conic body[2,27] illustrates the problem one would encounter in this case. It is unlikely that any support system can be found that will not have a significant interference effect on a short, blunt body, such as the Viking configuration.

Half-model testing is an alternative that avoids many of the support-interference effects discussed here. It has been shown to eliminate the problem of transition-augmented slender sting interference[38] (Fig. 20), and similar beneficial effects could be expected in regard to the support interference on

bulbous-based models. The problem is, of course, to account for the wall or mounting plate boundary layer and its effects on the near-wake flow of the model, the splitter plate problem discussed earlier, Fig. 16. Through careful selection of the gap between model and the wall or end plate, these boundary-layer effects can be minimized. One restriction of half-model testing is that it can only represent symmetric flow conditions. This automatically eliminates testing at high angles of attack, where flow asymmetries often occur.

The sting support interference becomes a problem when communication is opened up between the aft body and the base recirculation region, e.g., by a bulbous base at subsonic and transonic speeds, via boundary-layer transition at all speeds, and through the thickened body boundary layer in hypersonic low-density flow. There is another more general case which causes dynamic sting interference at all speeds, and that is when the body itself is engulfed in separated flow, as in the case of a blunt-nose cylinder-flare body at transonic speeds[60,60] (Fig. 33).

Although there may be no sting size small enough to eliminate all interference, it is, in many cases, possible to minimize the interference to an acceptable value by using a very slender sting support, as in Fig. 30. In so doing, however, one usually changes the testing from a single-degree-of-freedom (pitch only) to a two-degrees-of-freedom system (pitch and plunge).[62] For subcritical sting stiffness, the result is that the measured damping is increased for a slender body (with $C_{l\alpha} > 0$).[62] If one measures the sting plunging, it is relatively easy to correct for its effect on the measured stability derivatives. This is especially true for linear aerodynamic characteristics.[63,64] It can also be done in the case of highly nonlinear moment characteristics, provided that the lift characteristics can be approximated by a linear segment for the α range of interest for each data point.[62]

There is one case for which this two-degrees-of-freedom testing of a sting-supported model is the only means, short of free flight, that can provide a reasonable measurement of the dynamic stability derivative. The case in point is dynamic tests of short, blunt bodies such as the Viking configuration (Fig. 18). By varying the sting diameter down to very small sizes, an assessment of the interference for a finite-size sting could be made. The problem of the interference for a zero-size sting still remains. However, as $C_{l\alpha} > 0$ for short, blunt bodies, the sting plunging will produce a dynamically destabilizing influence.[62] Thus it is much less likely that measurements with a very slender sting will produce an unconservative (too damped) measurement of the blunt body dynamic stability.

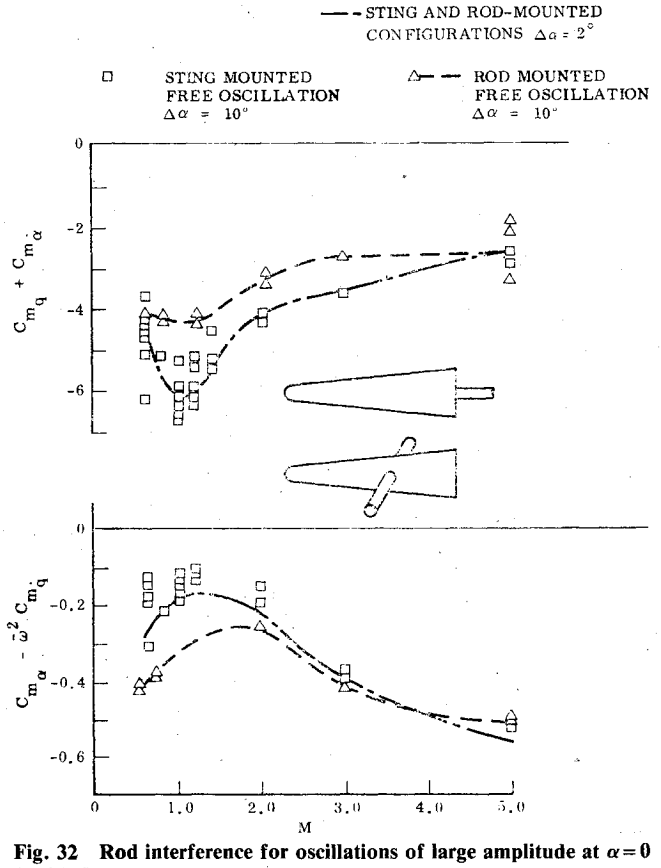

Fig. 32 Rod interference for oscillations of large amplitude at $\alpha = 0$ (Ref. 16).

High-α Testing

The complications arising in flight at high angles of attack were discussed extensively in a recent AGARD meeting.[65] One of the conclusions drawn from the meeting[66,67] was that the interference effects from the large, bulky support systems used in high-alpha testing needed to be investigated. According to an extensive survey of dynamic testing techniques,[68] the support systems shown in Fig. 34 are typical. It is obvious that these support systems will interfere with the separated flow vortices and wakes shed from the model, as is pointed out in Ref. 67. Only two papers in the AGARD conference addressed this problem by comparing the wind tunnel data with free-flight results for combat aircraft[69,70] (Fig. 35). It can be seen that significant differences between

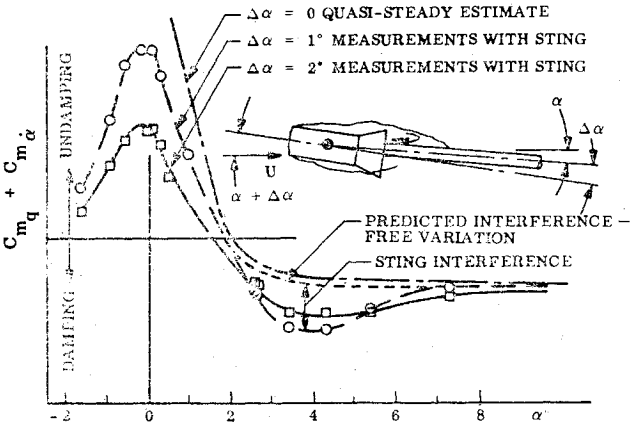

Fig. 33 Effect of cylindrical sting on the damping of a cylinder-flare body at $M = 0.65$.

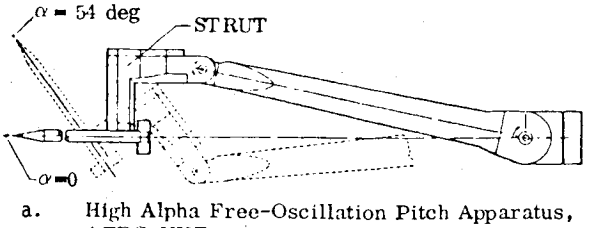

a. High Alpha Free-Oscillation Pitch Apparatus, AEDC-VKF

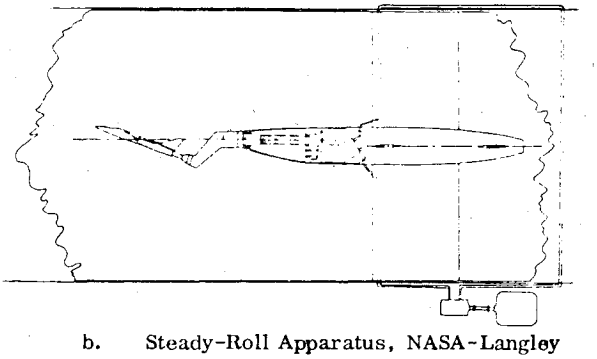

b. Steady-Roll Apparatus, NASA-Langley

Fig. 34 High-alpha model support systems (Ref. 68).

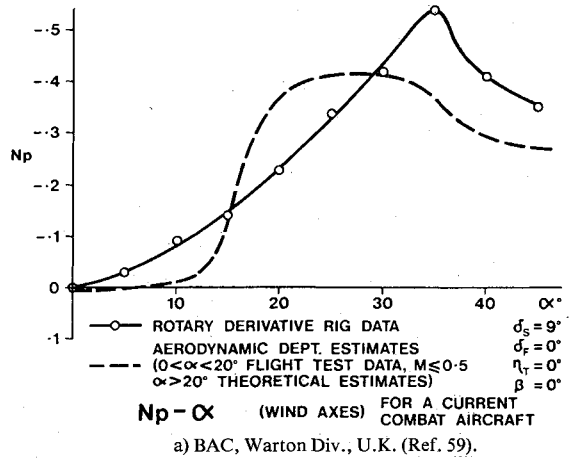

a) BAC, Warton Div., U.K. (Ref. 59).

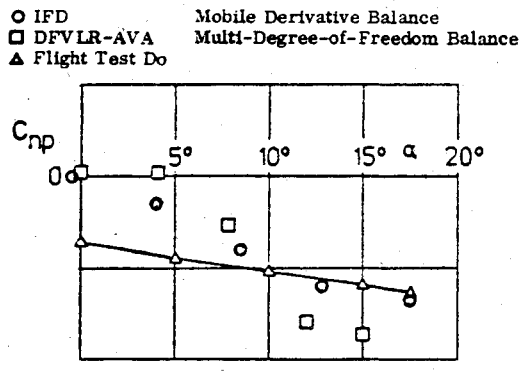

b) DFVLR, West Germany (Ref. 60).

Fig. 35 Comparison of side moment characteristics measured in wind tunnel and obtained in flight.

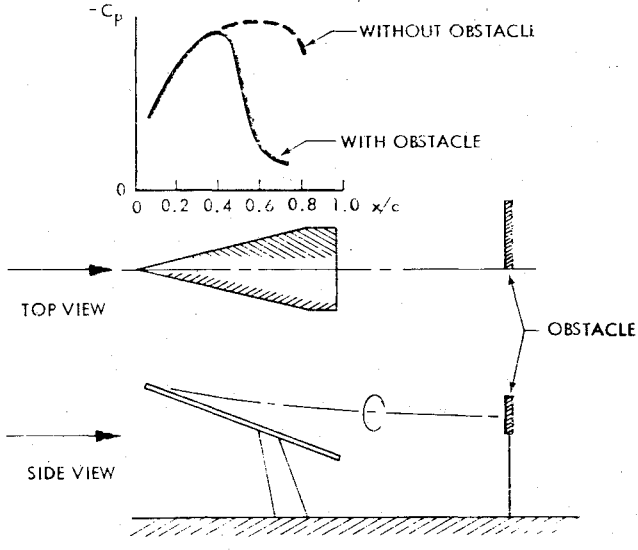

Fig. 36 Vortex burst on a 75-deg delta wing caused by downstream obstacles (Ref. 71).

wind tunnel and flight test results exist already at moderate angles of attack. One likely cause for the deviations is support interference, while wind tunnel wall interference and Reynolds number mismatch represent other possibilities.

How powerfully the support interference can affect the shed vortices is illustrated by Hummel's results[71] (Fig. 36). An obstacle placed one (center) chord length downstream of the trailing edge, on one-half of a 76-deg swept delta wing, causes the vortex breakdown to move from 80 to 40% chord, thereby changing the wing loading extensively. Hummel's experiment was recently repeated for a 70-deg arrow wing.[72]

Figure 37 shows the lateral stability characteristics measured by two different support systems.[72] Although only

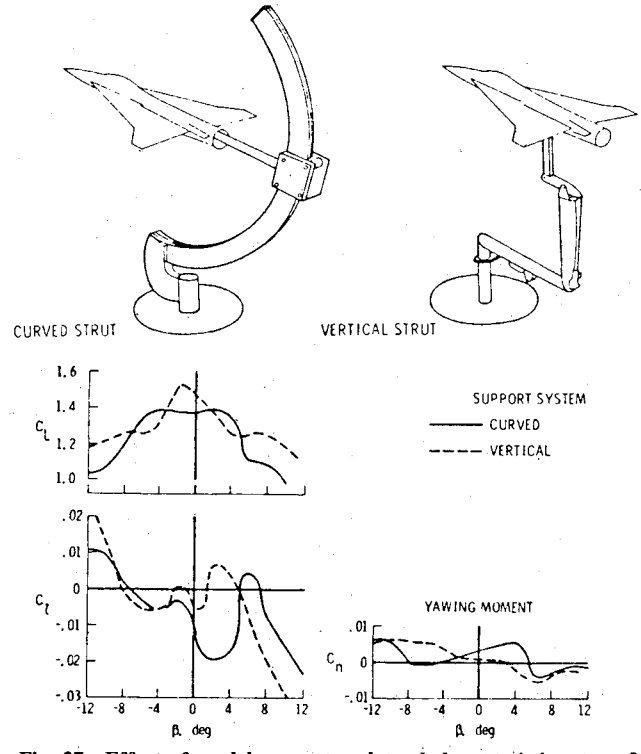

Fig. 37 Effect of model support on lateral characteristics at $\alpha = 35$-deg (Ref. 72).

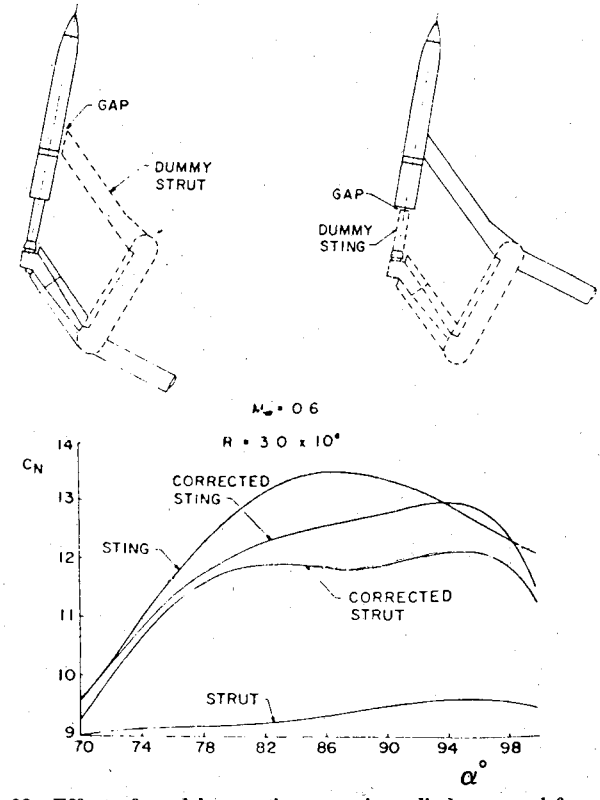

Fig. 38 Effect of model mounting on ogive-cylinder normal force characteristics at high angles of attack (Ref. 75).

the curved strut is likely to cause early vortex burst, the vertical strut support can have its own interference effect according to results for a swept-wing/ogive-cylinder configuration.[25] This could, of course, be the strut-body interference to be discussed shortly. However, the leeward side separated flow on highly swept delta wings can be very sensitive to disturbances on the windward side, as is demonstrated by Lambourne's results.[73] In the thorough

calibration of the test setup it was discovered that the pressure transducer housing, protruding slightly from the bottom surface, could cause a severe disturbance of the lee side vortex flow, if placed near the leading edge.

A wire attachment on the underside of a wing could have a similar effect. A strut could distort the windward side flow, especially at nonzero angles of sideslip, thereby affecting the lee side vortex shedding. Winkelmann[74] has shown that even for a straight wing a windward side strut can have a dramatic effect on the lee side separated flow pattern.

The problem of strut interference on bodies at high angles of attack has been demonstrated.[75] By testing with a dummy strut, the results in Fig. 38 were obtained showing the severe support interference caused by the leeward side strut support. The similarity between the lee side strut effect and the effect of splitter plate on the vortex shedding from a cylinder in two-dimensional flow has been pointed out.[76] As the splitter plate interferes with the cross-wake communication necessary for Karman vortex shedding, so the strut interferes with the steady counterpart, the asymmetric vortex shedding from a slender body at high angles of attack.[77-79] Miniscule windward side blowing has a very large effect on the asymmetric vortex shedding from an inclined slender body, as is evidenced by the measured side moment.[80] In view of this, it is not hard to visualize that a windward side strut support also can interfere strongly with the body vortex shedding.

Conclusions and Recommendations

A review of support-interference effects on measured stability derivatives reveals the following:

1) All support systems cause interference of one kind or another.

2) Support interference is much more of a problem in dynamic than in static tests.

3) Support interference is increased greatly by the presence of a boat-tail or dome-shaped base and, at transonic speeds, even by modest base-shoulder roundness.

4) The support interference is particularly a problem at transonic and hypersonic Mach numbers.

5) When boundary-layer transition occurs near the base, on the aft body, or in the wake, the problem of support interference is aggravated greatly.

6) In high-α tests, all strut supports cause significant interference.

The following steps will avoid or greatly minimize the effects of support interference:

1) Asymmetric sting or sting-strut supports should be avoided.

2) In tests of slender bodies with bulbous bases at low angles of attack, the transverse rod mount should be used.

3) In tests at moderate to high angles of attack, the slender, symmetric sting causes little support interference.

4) In many cases, half-model testing provides the means to avoid troublesome support interference.

5) When the model consists of a short, bulbous-based body, using a very slender sting and, if possible, measuring the sting plunging provide the best testing means short of free flight.

6) In difficult cases when the true dynamic stability characteristics cannot be ascertained from measurement with only one type of support system, combining half-model testing with tests of rod- or sting-mounted models should provide the information needed to bound the true dynamic stability derivative.

Acknowledgement

The authors are indebted to Nancy Tingas for her help with the manuscript. The paper is based upon material presented in Ref. 81

References

[1]Perkins, E. W., "Experimental Investigations of the Effects of Support Interference on the Drag of Bodies of Revolution at a Mach Number of 1.5," NACA TN 2292, Feb. 1951.

[2]Whitfield, J. P., "Support Interference at Supersonic Speeds," AGARD Rept. 300, March 1959.

[3]Kavanau, L. L., "Base Pressure Studies in Rarefield Supersonic Flow," *Journal of Aerospace Sciences*, Vol. 23, March 1956, pp. 193-207.

[4]Chapman, D. R., Kuehn, D. M., and Larson, H. K., "Investigation of Separated Flows in Supersonic and Subsonic Streams With Emphasis on the Effect of Transition," NACA TN 3869, Dec. 1957.

[5]Needham, D. A., and Stollery, J. L., "Boundary Layer Separation in Hypersonic Flow," AIAA Paper 66-455, June 1966.

[6]Nash, J. F., "Analysis of Two-Dimensional Turbulent Base Flow, Including the Effect of the Approaching Boundary Layer," National Physics Laboratory, Great Britain, NPL Aero Rept. 1035, July 1962.

[7]Love, E. S., "Base Pressure at Supersonic Speeds on Two-Dimensional Airfoils and on Bodies of Revolution With and Without Fins Having Turbulent Boundary Layers," NACA TN-3819, Jan. 1957.

[8]Lee, G. and Summers, J. L., "Effects of Sting-Support Interference On the Drag of an Ogive-Cylinder Body at 0.6 to 1.4 Mach Number," NACA RM A 57109, Dec. 1957.

[9]Uselton, B. L., and Cryan, F. B., "Critical Sting Length as Determined by the Measurement of Pitch-Damping Derivatives for Laminar, Transitional and Turbulent Boundary Layers at Mach Number 3 for Reduced Frequencies of 0.0033 and 0.0056," AEDC TR-77-66, July 1977.

[10]Uselton, B. L., "Sting Effects as Determined by the Measurement of Pitch Damping Derivatives and Base Pressures at Mach Number 3," AIAA Paper 78-830, April 1978.

[11]Uselton, B. L., and Cryan, F. B., "Sting Interference Effects as Determined by Measurements of Dynamic Stability Derivatives, Surface Pressure and Base Pressure for Mach Numbers 2 through 8," AEDC TR-79-89, Oct. 1980.

[12]Cryan, F. B., Uselton, B. L., and Marquart, E. J., "Evaluation of Critical Sting Length on a 7-degree Cone as Determined by Measurements of Dynamic Stability Derivatives and Base Pressure for Mach Numbers 0.2 through 1.3," AEDC TR-80-17, Jan. 1981.

[13]Stivers, L. S. Jr. and Levy Lionel, L. Jr., "Effects of Sting-Support Diameter on the Base Pressures of an Elliptic Cone at Mach Numbers from 0.60 to 1.40," NASA TN D-354, Feb. 1971.

[14]Sieling, W. R., "The Effect of Sting Diameter and Length on Base Pressure at $M=3.88$," *The Aeronautical Quarterly*, Vol. 19, Nov. 1967, pp. 368-374.

[15]Cresci, R. J. and Schmidt, E. M., "Near Wake Measurements in the Pressure of an Instrumentation Boom," PIBAL Report 1034, Polytechnic Institute of Brooklyn, Farmingdale, New York, Nov. 1967.

[16]Ericsson, L. E. and Reding, J. P., "Aerodynamic Effects of Bulbous Bases," NASA CR-1339, Aug. 1969.

[17]Foster, A. D., "A Compilation of Longitudinal Aerodynamic Characteristics Including Pressure Information for Sharp-and Blunt Nose Cones Having Flat and Modified Bases," Sandia National Laboratories, Livermore, Calif., SANDIA SC-R-64-1311, Jan. 1965.

[18]Iversen, J. D., "Base and Surface Pressure Variation with Mach Number on a Right Circular Cone," Sandia National Laboratories, Livermore, Calif., SANDIA SCTM 202-56-51, Sept. 1956.

[19]Robertson, J. E. and Chevalier, H. L., "Characteristics of Steady-State Pressures on the Cylindrical Portion of Cone-Cylinder Bodies at Transonic Speeds," AEDC TDR-63-104, Aug. 1963.

[20]Ericsson, L. E., "Steady and Unsteady Terminal-Shock Aerodynamics on Cone-Cylinder Bodies," NASA CR-61560, Oct. 1967.

[21]Woods, P. and Ericsson, L. E., "Aeroelastic Considerations in a Slender Blunt-Nose Multistage Rocket," *Aerospace Engineering*, Vol. 21, May 1962, pp. 42-51.

[22]Ericsson, L. E.,, "Aerolastic Instability Caused by Slender Payloads," *Journal of Spacecraft and Rockets*, Vol. 4, Jan. 1967, pp. 65-73.

[23]Rubin, D. V., "Effects of Lateral Support Strut on Body Pressure Distributions at Transonic Speeds," AOMC RD-TR-72-6, U.S. Army Missile Command, Redstone Arsenal, Ala., Jan. 1972.

[24]Hammond, D. G. and Wilkerson, C. Jr., "An Evaluation of Single and Multiple Sting Support Methods to Obtain Modified Interference-Free Wind Tunnel Data," AIAA Paper 71-267, March 1971.

[25]Brännström, B. and Lindaw, O., "Investigations of Interference Effects In a Wind Tunnel From a Model Support Strut on a Reflection-Plane Mounted Half Model," The Aeronautical Research Institute of Sweden, FFA Tech. Note AU-1335, 1978.

[26]Finnerly, C. S., "A Parametric Study of Support System Interference Effects on Nozzle/Afterbody Throttle Dependent Drag in Wind Tunnel Model Testing," AIAA Paper 79-1168, June 1979.

[27] Gray, J. D., "Base-Pressure Measurements With Wire Supported Models at Supersonic Speeds," AEDC TN-61-23, March 1961.

[28] Orlik-Rückemann, K. J., "Dynamic Stability Testing of Aircraft-Needs Versus Capabilities," *Progress in Aerospace Sciences,* Vol. 16, No. 4, Pergamon Press, New York, 1975, pp. 431-447.

[29] Reding, J. P. and Ericsson, L. E., "Dynamic Support Interference," *Journal of Spacecraft and Rockets,* Vol. 9, July 1972, pp. 547-553.

[30] Wehrend, W. R. Jr., "An Experimental Evaluation of Aerodynamic Damping Moments on Cones With Different Centers of Rotations," NASA TN-D-1768, March 1963.

[31] Uselton, B. L., and Wallace, A. R., "Damping-in-Pitch and Drag Characteristics of the Viking Configuration at Mach Numbers From 1.6 through 3," AEDC TR-72-56, May 1972.

[32] Steinberg, S., Uselton, B. L., and Siemers II, P. M., "Viking Pitch Damping Derivatives as Influenced by Support Interference and Test Techniques," *Journal of Spacecraft and Rockets*, Vol. 10, July 1973, pp. 443-449.

[33] Stivers, L. S. Jr., "Effects of Sting on the Supersonic Force Moment Characteristics of an Apollo Model at Angles From −30 deg to +185 deg," NASA TMX-1081, March 1965.

[34] Trescot, C. D. Jr., Brown, C. A. Jr., and Howell, D. T., "Effects of Reynolds Number and Model Support on the Supersonic Aerodynamic Characteristics of a 140-deg Included Angle Cone," NASA TMX-3019, July 1974.

[35] Ericsson, L. E. and Reding, J. P., "Transonic Sting Interference," *Journal of Spacecraft and Rockets,* Vol. 17, March-April 1980, pp. 140-144.

[36] Yanagizawa, M., "Measurement of Dynamic Stability Derivatives of Cones and Delta-Wings at High Speed," National Aerospace Laboratory, Tokyo, Japan, NAL TR-172, 1969.

[37] Liu, D. D., Platzer, M. F., and Ruo, S. Y., "On the Calculation of Static and Dynamic Stability Derivatives for Bodies of Revolution at Subsonic and Transonic Speeds," AIAA Paper 70-190, New York, N.Y., Jan. 1970.

[38] Orlik-Rückemann, K. J., LaBerge, J. G., and Inyengar, S., "Half-and-Full Model Experiment on Slender Cones at Angle of Attack," *Journal of Spacecraft and Rockets,* Vol. 10, Sept. 1973, pp. 575-580.

[39] Adcock, J. B., "Some Experimental Relations Between the Static and Dynamic Stability Characteristics of Sting-Mounted Cones With Bulbous Base," *Transactions of the 3rd Technical Workshop on Dynamic Stability Problems,* Paper 5, Vol. II, NASA Ames R. C., Moffett Field, Calif., Nov. 1968.

[40] Jecmen, D. M., Reding, J. P., and Ericsson, L. E., "An Application of Automatic Carpet Plotting to Wind Tunnel Data Reduction," *Journal of Spacecraft and Rockets,* Vol. 4, March 1967, pp. 408-410.

[41] Hama, F. R., "Experimental Studies of the Lip Shock," *AIAA Journal,* Vol. 6, 1968, pp. 212-219.

[42] Hobbs, R. B. Jr., "Hypersonic Dynamic Stability, Part II, Conical Body Experimental Programs," AFFDL TDR-64-149, Part II, Jan. 1967.

[43] Hobbs, R. B. Jr., private communication of sting geometry, 1968.

[44] Walchner, O. and Clay, J. T., "Nose Bluntness Effects on the Stability Derivatives of Cones in Hypersonic Flow," *Transactions of the 3rd Technical Workshop on Dynamic Stability Problems,* Paper 5, Vol. II, NASA Ames Research Center, Moffett Field, Calif., Nov. 1968.

[45] Walchner, O., private communication of unpublished data on hypersonic dynamic support interference, June 1968.

[46] Slattery, R. E., Clay, W. G., and Stevens, R. R., "Interactions Between a Hypersonic Wake and a Following Hypersonic Projectile," *AIAA Journal,* Vol. 1, April 1963, pp. 974-975.

[47] Walchner, O., Sawyer, F., Quinn B., and Friberg, E., "Hypersonic Stability Derivatives for a Standard 10 Degree Cone," ARL 67-0099, Aerospace Research Laboratories, Wright Patt. AFB, Ohio, May 1967.

[48] Welsh, C. J., Winchenbach, G. L., and Madigan A. N., "Free-Flight Investigation of the Aerodynamic Characteristics of a Cone at High Mach Numbers," *AIAA Journal,* Vol. 8, Feb. 1970, pp. 294-300.

[49] Ericsson, L. E. and Reding, J. P., "Viscous Interaction or Support Interference – The Dynamicist's Dilemma," *AIAA Journal,* Vol. 16, April 1978, pp. 363-368.

[50] Morrison, A. M., Holmes, J. E., and Lawrence, W. R., "An Investigation of the Damping in Pitch Characteristics of a Ten Degree Cone, Naval Surface Weapons Center, White Oak, Md., NSWC/WOL/TR 75-84, June 1975.

[51] Urban, R. H., "A Dynamic Stability for Hypervelocity (Hot-Shot) Tunnels," AEDC TR-65-222, Oct. 1965.

[52] Urban, R. H., and Shanahan, R. J., "Dynamic Stability Characteristics of a 10 Degree Cone at Mach Number 20," AEDC TR-65-80, April 1965.

[53] Schueler, C. J. and Ward, L. K., and Hodapp, A. E. Jr., "Techniques for Measurement of Dynamic Stability Derivatives in Ground Test Facilities," AGARDograph 121, Oct. 1967.

[54] Uselton, J. C. and Uselton, B. L., "Validity of Small-Amplitude Oscillation Dynamic-Stability Measurement Technique," *Journal of Spacecraft and Rockets,* Vol. 13, May 1976, pp. 266-270.

[55] Wehrend, W. R., "A Wind-Tunnel Investigation of the Effect of Changes in Base Contour on the Damping in Pitch of a Blunted Cone," NASA TND-2067, Nov. 1963.

[56] Compton, W. B. III, "Effect on Base Drag of Recessing the Bases of Conical Afterbodies at Subsonic and Transonic Speeds," NASA TND-4821, Oct. 1968.

[57] Ericsson, L. E., "Correlation of Attitude Effects on Slender Vehicle Transition," *AIAA Journal,* Vol. 12, April 1974, pp. 523-529.

[58] Dayman, B. Jr., "Optical Free-Flight Wake Studies," Jet Propulsion Laboratory, Pasadena, Calif., JPL TR 32-364, Nov. 1962.

[59] Rakich, J. V. and Cleary, J. W., "Theoretical and Experimental Study of Supersonic Steady Flow Around Inclined Bodies of Revolution," *AIAA Journal,* Vol. 8, March 1970, pp. 511-518.

[60] Reese, D. E. Jr. and Wehrend, W. R. Jr., "An Investigation of the Static and Dynamic Characteristics of a Series of Blunt-Nosed Cylinder Flare Models at Mach Numbers from 0.65 to 2.20," NASA TMX-110, Jan. 1960.

[61] Ericsson, L. E., "Separated Flow Effects on the Static and Dynamic Stability of Blunt Nosed Cylinder Flare Bodies," NASA CR-76919, Dec. 1965.

[62] Ericsson, L. E., "Effects of Sting Plunging on Measured Nonlinear Pitch Damping," AIAA Paper 78-832, April 1978.

[63] Burt, G. E. and Uselton, J. C., "Effects of Sting Oscillations on the Measurement of Dynamic Stability Derivatives," *Journal of Aircraft,* Vol. 13, March 1976, pp. 210-216.

[64] Canu, M., "Measure en Soufflerie de l'Amortissement Aerodynamique en Tanage d'une Maquette d'Avion Oscillant Suivant Deux Degres de Liberté," *La Récherche Aerospatiale,* Vol. 5, Sept./Oct. 1971, pp. 257-267.

[65] "Dynamic Stability Parameters," AGARD CP-235, Nov. 1978.

[66] Ericsson, L. E., "Technical Evaluation Report on the Fluid Dynamics Panel Symposium on Dynamic Stability Parameters," AGARD-AR-137, April 1979.

[67] Ericsson, L. E., "A Summary of AGARD FDP Meeting on Dynamic Stability Parameters," Paper 2, AGARD CP-260, Sept. 1978.

[68] Orlik-Rückemann, K. J., "Dynamic Stability Testing in Wind Tunnels," AGARD CP-235, Paper 1, Nov. 1978.

[69] Matthews, A. W., "Experimental Determination of Dynamic Derivatives Due to Roll at BAC, Warton," AGARD CP-235, Paper 4, Nov. 1978.

[70] Hafer, X., "Wind Tunnel Testing in Wind Tunnels Testing of Dynamic Derivatives in W. Germany," AGARD CP-235, Paper 5, Nov. 1978.

[71] Hummel, D., "Untersuchungen über das Aufplatzen der Wirbel an schlanken Delta Flügeln," *Zeitshrift fuer Flugwissenschaften,* Vol. 13, Heft 5, 1965, pp. 158-168.

[72] Johnson, J. L. Jr., Grafton, S. B., and Yip, L. P., "Explatory Investigation of Vortex Bursting on the High-Angle-of-Attack Lateral

Directional Stability Characteristics of Highly Swept Wings," AIAA Paper 80-0463, March 1980.
[73]Lambourne, N. C., Bryer, D. W., and Maybrey, J. F. M., "Pressure Measurements on a Model Delta Wing Undergoing Oscillatory Deformation," Aeronautical Research Council, Great Britain, NPL Aero Rep. 1314, March 1970.
[74]Winkelmann, A. E., "Flow Surveys of Separated Flow on a Rectangular Planform Wing," AIAA Paper 81-0255, Jan. 1981.
[75]Dietz, W. E. and Altstatt, M. C., "Experimental Investigation of Support Interference on an Ogive-Cylinder at High Incidence," *Journal of Spacecraft and Rockets,* Vol. 16, 1979, pp. 67-68; see also AIAA Paper 78-165, Jan. 1978.
[76]Nelson, R. C. and Mouch, T. N., "Cynlinder/Splitter-Plate Data Illustrating High-α Support Interference," *Journal of Spacecraft and Rockets,* Vol. 16, March-April 1979, pp. 126-128.
[77]Ericsson, L. E. and Reding, J. P., "Steady and Unsteady Vortex-Induced Asymmetric Loads on Slender Vehicles," *Journal of Spacecraft and Rockets,* Vol. 18, March-April 1981, pp. 97-109.
[78]Ericsson, L. E. and Reding, J. P., "Review of Vortex-Induced Asymmetric Loads – Part I," *Z. Flugwiss. Weltraumforschungs* Vol. 5, Heft 3, 1981, pp. 162-174.
[79]Ericsson, L. E. and Reding, J. P., "Review of Vortex-Induced Asymetric Loads – Part II," *Z. Flugwiss. Weltraumforschungs.* Vol. 5, Heft 6, 1981, pp. 349-366.
[80]Almosino, D. and Rom, J., "Alleviation of the Lateral Forces and Moments Acting on a Slender Body at High Angles of Attack Using Jet Injection at Subsonic and Transonic Speeds," AIAA Paper 80-1558, Aug. 1980.
[81]Ericsson, L. E., "Support Interference," Lecture 8, AGARD-LSP-114, March 1981.